

EFFECT OF BINDER TYPE AND MIXING WATER CHEMISTRY ON MICROSTRUCTURAL EVOLUTION OF CEMENTED PASTE BACKFILL

Serge Ouellet, Université du Québec en Abitibi-Témiscamingue, Rouyn-Noranda, Canada

Bruno Bussière, Université du Québec en Abitibi-Témiscamingue, Rouyn-Noranda, Canada

Mostafa Benzaazoua, Université du Québec en Abitibi-Témiscamingue, Rouyn-Noranda, Canada

Michel Aubertin, École Polytechnique, Montréal, Canada

Tikou Belem, Université du Québec en Abitibi-Témiscamingue, Rouyn-Noranda, Canada

ABSTRACT

Mercury intrusion porosimetry (MIP) tests were performed on 54 hardened cement paste (CP) ($w/c = 0.33$) and cemented paste backfill (CPB) ($w/c = 7$) samples. Three binders (PC type 10, PC T10-fly ash, PC T10-blast furnace slag) and three waters containing different sulphate proportions ($\approx 0, 4613, 7549$ ppm) were used in the specimen preparation process. Cement paste study showed microstructural differences between binders and to identify the main influence factors of the microstructural evolution before the porosimetry tests performed on cemented paste backfill samples. MIP results on CPB indicate that despite a constant total porosity, pore size diameter decreased with curing time. Pore refinement was more important with the slag binder, which would explain higher mechanical strength with this binder. Moreover, the effect of sulphate ions in mixing water was positive on pore refinement and on strength evolution. Tests showed a direct relationship between mechanical strength and pores refinement; and that MIP technique is an efficient tool to evaluate microstructure of CPB.

RÉSUMÉ

Des essais au porosimètre au mercure (PHg) ont été effectués sur 54 échantillons de pâte de ciment (PC) ($e/c = 0.33$) et de remblais en pâte cimentée (RPC) ($e/c = 7$). Les échantillons étudiés étaient constitués de trois liants (CP type 10, CP 10-cendre volante, CP type 10-laitier de haut-fourneau) et de trois eaux ayant chacune une teneur en sulfate différente (\approx nulle, 4613, 7549 ppm). L'étude au PHg des pâtes de ciment a permis de rehausser les différences microstructurales entre les 3 ciments et d'identifier les principaux paramètres d'influence de l'évolution microstructurale et ce, avant la réalisation des essais sur les remblais cimentés en pâte. Les résultats obtenus sur les RPC montrent que malgré une porosité totale constante, il y a une diminution de la taille des pores avec le curage. Le raffinement des pores est plus important avec le ciment au laitier, ce qui pourrait expliquer en partie les meilleures résistances mécaniques obtenues. Par ailleurs, la présence de sulfate dans l'eau de gâchage a un effet positif sur le raffinement des pores et le gain de résistance mécanique. Les essais ont montré qu'il existe un lien direct entre l'UCS et la finesse des pores, et que le PHg est un outil efficace pour investiguer la microstructure des RPC.

1. INTRODUCTION

Every year the mining industry produces a large amount of mill tailings. A part of the generated tailings can be stored in underground mines as a cemented paste backfill (CPB) to stabilize open stopes (e.g. Hassani and Archibald, 1998; Benzaazoua et al., 1999; Aubertin et al., 2002). CPB is a composite material made of a mixture of thickened tailings (at a pulp density between 75 to 85%), binders (such as Portland cement, fly ash, blast furnace slag or a combination) and water. The main benefits of underground paste backfill include a higher strength and lower operating costs (in most cases) compared to hydraulic fills (Hassani and Archibald, 1998). Moreover, the use of paste backfill reduces the amount of tailings that have to be sent to surface disposal facilities. This reduction decreases both the environmental impact and capital expenditures of the tailings facility. Because the mining industry in Canada and around the world increasingly uses CPB, a better knowledge of their microstructural characteristics and of the main influence factors affecting microstructure and strength (water quality and quantity; type and percentage of binder, grain size distribution and mineralogy of tailings, etc.) is needed to get a global understanding of such material.

Over the past few years, a few authors investigated the microstructure of CPB. Mitchell and Wong (1982) showed a relationship between porosity, cement content, and pulp density. They showed that the porosity of the backfill decreased when the cement content was increased from 4 to 12 %, and that thickening tailings (removing water) was one of the main parameters to reduce total porosity. Keren and Kajnian (1983) incorporated the porosity parameter in a study on the water percolation rate through hydraulic fills. Benzaazoua et al. (2000) and Belem et al. (2001) used mercury intrusion porosimetry (MIP) tests to investigate the porosity of CPB. Their results showed that the total CPB porosity was very close to that of an agglomerated tailings. Belem et al. (2001) also showed that the addition of binder (5%wt) reduces pore size significantly, which reduces the saturated hydraulic conductivity and increases the water retention properties of the CPB. Finally, le Roux (2004) performed different tests including mercury intrusion porosimetry to evaluate and compare the microstructure of in situ and laboratory prepared CPB. MIP results showed that field and laboratory samples have a similar pore size distribution.

This paper presents a comparative study of the microstructural evolution using mercury intrusion porosimetry (MIP) technique for different cement pastes

(CP) and cement paste backfills (CPB) at different curing times. Cement paste mixtures (binder and water only) were prepared to enhance the cementitious effects and to isolate interactions between the water and the binder. The mixtures studied were made from three typical binders used in the mining industry (at 5%wt) and three types of water containing different typical sulphate concentrations. It is a common practice in the mining industry to use recycled water in the CPB preparation. Depending on the ore and the mineralurgical process at the mine, this water can contain sulphate ions that play a role in the hydration process of binders, and can precipitate in the paste and possibly generate cracks and loss of strength (Subauste and Odler, 2002). To complete the study, uniaxial compressive strength (UCS) tests were performed on samples to show the link between porosity evolution and mechanical strength.

2. MATERIALS AND METHODS

2.1 Materials and samples preparation

Both CPB and CP were prepared in small batches in a 20 litres bucket and mixed for at least 5 minutes with a ½ inch electric drill using a paint mixer bit. The three binders used were a CAN3-A5-M77 PC type 10 cement (T10) (100%), a mix of 20% PC T10 and 80% blast furnace slag (T10SL), and a mix of 70% PC T10 and 30% fly ash (T10FA). Table 1 presents the chemistry of binders (ICP-AES analysis) and some physical properties. The PC T10 binder showed a typical chemistry for this type of cement (Neville, 1981) and the calculated Bogue's composition is 64.4% for C3S, 6.6% for C2S, 8.7% for C3A and 7.4% for C4AF. According to ASTM C618-00 standard, the studied fly ash can be classified as a class C with a cumulative value for SiO₂, Al₂O₃ and Fe₂O₃ less than 70% and a SO₃ content less than 5%. BF slag met the recommendation of Malhotra (2001) to prevent sulphate attack with an Al₂O₃ percentage less than 11%. BF slag shows also the highest BET specific surface with a value of 21 380 cm²/g indicating that the size of particles was the finest of all binders. The specific surfaces of the other two binders are 12 764 and 8 697 cm²/g for OPC T10 and Fly ash respectively.

The mixtures used three different types of water: the first one was deionised by filtration (named W0), the second one was a mine water sampled at a backfill plant which contained a sulphate concentration of 4613 ppm (named W1), and the last one was also a mine water sampled at the backfill plant of a second mine which had a sulphate concentration of 7549 ppm (named W2). One can see in Table 2 that the calcium content of mine waters are relatively high (803 and 1790 ppm for W1 and W2 respectively). These high concentrations are mainly due to the ore processing techniques that use lime in the process to increase the pH. Alkali concentrations are relatively high but only the W1 water exceeded the recommended maximum concentration of 500 ppm Na₂O equivalent¹

from ASTM-C94 standard with a value of 1266.2 ppm Na₂Oeq. The W2 water had a Na₂Oeq. concentration of 187.7 ppm. The pH varied for the different waters between 4.57 to 9.62. Mine waters were filtered to remove suspended particles before analysis and mixing.

Table 1. Chemical composition of binders (ICP analysis)

	OPC T10 (%wt)	Fly ash (%wt)	BF Slag (%wt)
SiO ₂	19.25	44.93	36.37
Al ₂ O ₃	4.82	17.67	10.28
Fe ₂ O ₃	2.42	6.09	0.51
CaO	60.59	15.39	31.34
MgO	2.19	2.95	11.18
K ₂ O	0.81	0.65	0.48
Na ₂ O	2.10	7.41	2.01
SO ₃	3.92	1.90	3.20
D _r	3.12	2.53	2.91
SS BET (cm ² /g)	12764	8697	21380

Table 2. Chemical composition of waters (ICP analysis)

	W0 (ppm)	W1 (ppm)	W2 (ppm)
Al	0.03	1.06	0.29
Ca	0.02	803.00	1790.00
Cu	<0.01	0.59	0.21
Fe	0.05	0.04	1.01
K	0.14	41.40	48.00
Mg	0.01	1.00	1.71
Na	<0.2	915.00	111.00
Si	3.78	0.82	0.50
Zn	<0.02	0.08	0.53
SO ₄ ²⁻	0.36	4613.22	7548.91
pH	6.09	9.62	4.57
EhN	435.8	243.7	361.1
Cond. (µS/cm)	2	5950	3740

For all CPB mixtures ground silica from BEI Pecal was used to simulate tailings. The silica contains 99.76% SiO₂ and has a grain size distribution (evaluated with a laser Mastersizer from Malvern Instruments) close to the average of 11 mine tailings (coming from the province of Quebec and northern Ontario) with a percentage passing 80 µm of approximately 80% and a percentage of particles less than 2 µm of about 10% (Figure 1). The uniformity coefficient ($C_U = D_{60}/D_{10}$) and the coefficient of curvature ($C_C = D_{30}^2/D_{60} \cdot D_{10}$) are respectively 16.5 and 3.4. According to USCS classification the silica material can be classified as a non plastic silt (ML).

A total of 108 CPB and CP cylinders of 10 cm long and 5 cm in diameter were cured at room temperature and at a relative humidity greater than 75%. The binder proportion for the CPB was 5% by weight of dry silica. Water to cement ratios were 7 for the CPB mixtures (representing a water to solid ratio of 0.33) and 0.33 for the CP samples. Two cylinders of each mixture were cast to evaluate the uniaxial compressive strength (UCS) after 14, 43 and 92 curing days using a MTS 10/GL press with a 50kN capacity. After the UCS test was performed, a fraction of each cylinder was sampled (about 20 g) for the microstructural characterization.

¹ Na₂Oeq. = Na₂O + 0.658K₂O

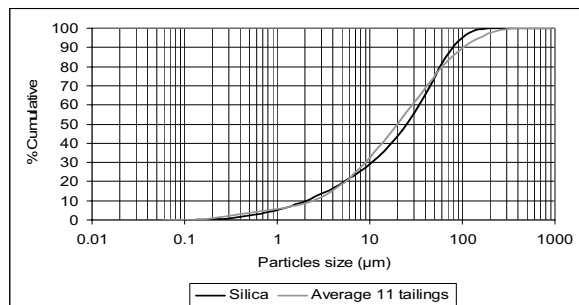


Figure 1, Particles size distribution of silica.

Drying of the samples was performed by a combination of freeze drying and oven drying. Samples were first cut in small cubes of about 1 cm³ each and immersed for more than 5 minutes in liquid nitrogen. Samples were then dried for a period of 24 hours at 7 mTorr and -50°C in a Virtis Ultra 35 Super XL freeze dryer. Immersion in liquid nitrogen allows solidifying rapidly the internal water in microcrystals of ice. The second step in the vacuum freeze dryer directly sublimates the ice without returning to a liquid phase. Another period of 24 hours in an oven at 45°C completed the drying; according to Kjellsen (1996) this should complete the drying without generating cracks. After the drying steps, all CP and CPB samples were maintained in a desiccator to avoid rehydration. Freeze drying technique, as the one used in this study, is considered a gentle drying technique that has been applied for many years on cement pastes (Gallé, 2001; Kjellsen, 1996) and on clayey soils (Hueckel et al., 1997; Simms and Yanful, 2001). Trying to keep the microstructure of a cement material as close as possible to the original microstructure is important. Oven drying at a too high temperature can cause cracks (Gallé, 2001) and remove water physically adsorbed and/or chemically attached on some hydrated minerals (Ramachandran and Beaudoin, 2001).

2.2 Mercury intrusion porosimetry

Mercury intrusion porosimetry (MIP) is based on the capillary law governing the penetration of a liquid into pores (Ramachandran and Beaudoin, 2001). For the case of a non-wetting liquid like mercury and a material with cylindrical pores, this law is expressed by the Washburn equation (e.g. :

$$D = -\left(\frac{1}{P}\right) 4\gamma \cos\phi, \quad (1)$$

where D is pore diameter, P the applied pressure, γ the surface tension and ϕ the contact angle.

According to MIP test theory, when a pressure is applied to a porous media surrounded by mercury, the mercury should fill the pores of a diameter equal to the pressure applied in respect to Washburn relation. The main limitation of the MIP test is related to the ink bottle effect. Because mercury must pass through the narrowest pores connecting the pore network, MIP cannot provide a true pore size distribution (Cook and Hover, 1999). Many papers were written on the evaluation of cement paste

porosity by MIP technique. Winslow and Diamond (1970) studied parameters influencing MIP and defined the parameter named "threshold diameter" that corresponds to the diameter, according to Washburn's equation, where the maximum of mercury fills the sample. The significance of this parameter was explained by the authors to be the minimum diameter of pores which are geometrically continuous throughout the cement paste sample. Later, Diamond (2000) concluded that the MIP misallocated the sizes of almost all of the volume of pores in hydrated cementitious materials. However, he mentioned that the MIP was a technique with a good repeatability and when used on a comparative basis was able to give valid information on permeability, ions transport and total porosity in cement systems. Other authors (Cook and Hover, 1999; Wild, 2001; Chatterji, 2001; Gallé, 2003) added that monitoring the threshold diameter evolution over the curing time is a useful technique that reflects the pore refinement within the cement paste. Based on the available literature it can be said that MIP is a reliable qualitative test to evaluate the microstructure evolution of cemented materials if the limitations of the technique are taken into account.

In this study MIP tests were performed on CP and CPB samples after each curing period. The equipment used is an Autopore III 9420 from Micromeritics that can generate a maximum pressure of 414 MPa and evaluate a theoretical pore diameter of 0.003 μm. The contact angle and surface tension assumed for all tests were respectively 130° and 485 dynes/cm. Depending on the average porosity, the samples were cut in small cubes between 0.6 and 3 grams to reach the manufacturer recommendation of mercury stem volume between 25 and 90%.

3. MIP RESULTS AND ANALYSIS

Cemented paste backfill is a material with a low cement content and a high water/cement ratio. Usually about 5% of binder by weight of dry tailings is added and a water/cement ratio of 7 is used. In these conditions it is difficult to isolate and study the cementitious matrix. Keeping in mind that the evolution of the CPB over time is controlled by the binder, mixtures of cement paste (binder and water only) were prepared to enhance the cementitious effects and to allow the observation of the water and binder behaviour on the microstructure of CPB. In addition, because literature on cement paste is abundant, the tests on CP samples were used to validate the research protocol and MIP results.

3.1 Cement pastes

Figures 2 to 7 present MIP pore size distribution of CP mixed with waters W0 and W2 (results using W1 water are not shown here but exhibit the same behaviour). In these graphs, the sum of porosity for each increment of pressure corresponds to the CP total porosity. Table 3 and 4 present respectively the total porosity and the threshold diameter for all CP mixtures. Let's recall that the threshold diameter corresponds to the pore diameter

where the highest rate of mercury intrusion occurs in the CP.

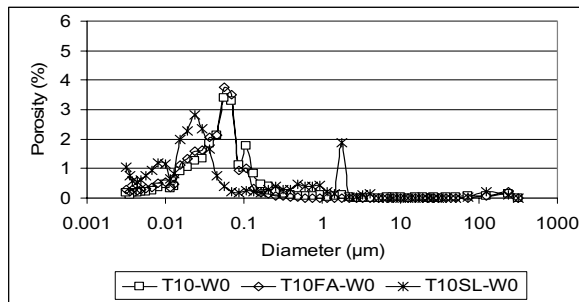


Figure 2, MIP results at 14 days with W0 water

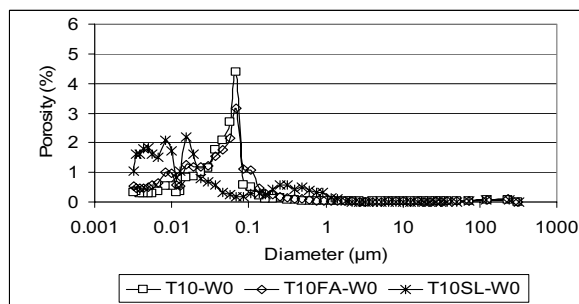


Figure 3, MIP results at 43 days with W0 water

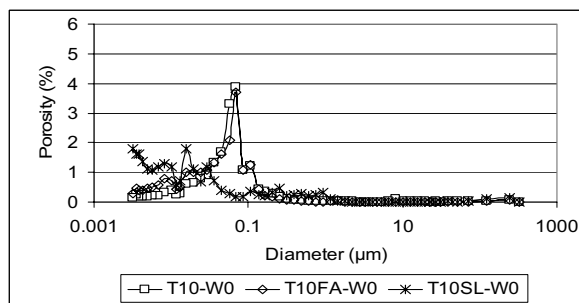


Figure 4, MIP results at 92 days with W0 water

3.1.1 Effect of binders

Figures 2 to 4 show that CP samples with T10SL binder exhibit a different behaviour than the CP samples using T10 and T10FA. First, the position of the highest mercury intrusion (threshold diameter) is at the left side of the graph (smaller pore size), compared with the other two. This means that pastes using T10SL need more pressure to be intruded by the mercury, indicating a finer porosity. Another particularity of T10SL CP samples is the small intrusion at a diameter near 1 μm . This may well imply that these pastes have two families of pores: a small one near 1 μm and another (the main one) usually below 0.1 μm . CP mixtures with T10 and T10FA binders show similar intrusion behaviour and seem to have similar microstructures. CP mixtures using the T10SL binder show significant changes of threshold diameter. For these samples, the threshold diameter drops by about one half

from 14 to 92 days (Table 4), while it stays relatively unchanged for CP using T10 and T10FA.

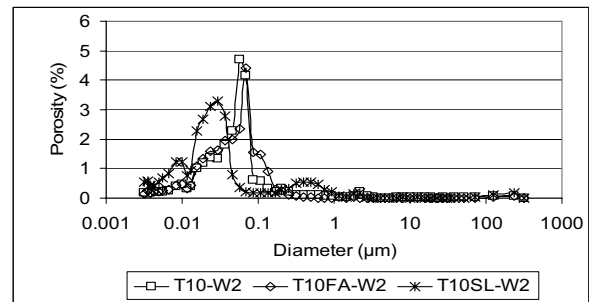


Figure 5, MIP results at 14 days with W2 water

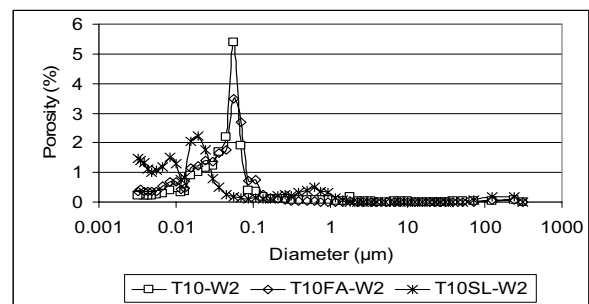


Figure 6, MIP results at 43 days with W2 water

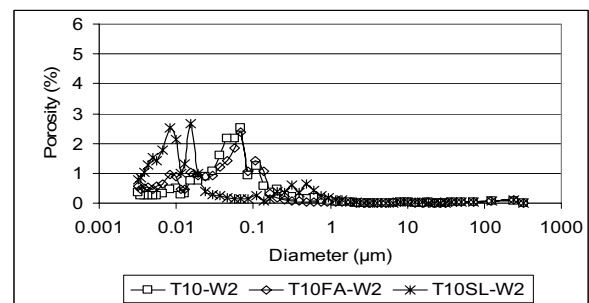


Figure 7, MIP results at 92 days with W2 water

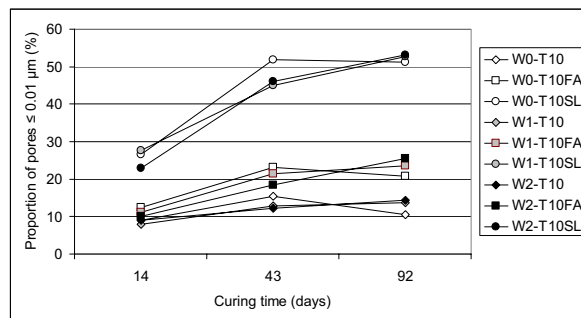
Another interesting aspect of T10SL pastes is that at all curing times, the total porosity is higher than that of the other pastes, even if the pore size distribution is finer. To illustrate the differences within pastes, Figure 8 shows the sum of pores $\leq 0.01 \mu\text{m}$ (corresponding to an intrusion pressure of 137 MPa and higher). This sum corresponds to the porosity associated to each increment of pressure for pore size less or equal to 0.01 μm . The difference between binders is highlighted in this figure. Mixtures with T10SL binder show a higher proportion (more than 50% after 92 days), but the mixtures with T10FA binder show a difference with T10 samples (between 21 and 25% for T10FA vs 11 to 14% for T10). This difference could be produced by a late hydration of FA particles and a pozzolanic effect.

Table 3, CP's total MIP porosity (%)

	14 days	43 days	92 days
W0-T10	23.87	21.09	20.07
W0-T10FA	24.40	24.49	22.38
W0-T10SL	28.33	28.59	23.99
W1-T10	23.39	20.88	18.24
W1-T10FA	25.45	23.10	23.01
W1-T10SL	26.73	25.96	24.17
W2-T10	24.31	20.78	20.37
W2-T10FA	24.67	22.50	21.89
W2-T10SL	28.52	24.74	25.03

Table 4, Paste's threshold diameters (μm)

	14 days	43 days	92 days
W0-T10	0.0565	0.0698	0.0698
W0-T10FA	0.0565	0.0697	0.0698
W0-T10SL	0.0237	0.0155	0.0154
W1-T10	0.0697	0.0566	0.0454
W1-T10FA	0.0697	0.0566	0.0565
W1-T10SL	0.0237	0.0191	0.0082
W2-T10	0.0565	0.0565	0.0697
W2-T10FA	0.0699	0.0565	0.0696
W2-T10SL	0.0294	0.0191	0.0155

Figure 8, Evolution of porosity $\leq 0.01 \mu\text{m}$ (137 MPa)

3.1.2 Effect of curing time

All CP samples show a slight decrease of the total porosity with the curing period (Tables 3). Figures 2 to 4 present an increase in the porosity under $0.01 \mu\text{m}$ with curing time for all binders. The same behaviour is observed in figures 5 to 7 (CP with W2 water). Results presented in Figure 7 (MIP results at 92 days with W2 water) show a clear difference in the maximum intrusion values, which are all below 3% porosity. This means that there is a better distribution of the pore size in the matrix (on the finer side), with fewer large size families.

3.1.3 Effect of mixing water quality

Figure 8 also shows the influence of water quality. For the curing time of 43 days and 92 days, the percentage of pores corresponding to a diameter $\leq 0.01 \mu\text{m}$ decreases or stays the same for samples with W0 water, but continues to rise slowly for mixtures containing sulphated water. This could indicate the precipitation of sulphated minerals in the mid to large size pores, contributing to an increase in the number of pores under $0.01 \mu\text{m}$.

3.2 Cemented paste backfills

MIP tests on CP samples highlighted the influence of some factors (binder type, water type, curing time) on MIP porosity results. Other tests on CPB samples have been performed to evaluate if observations on CP samples are still valid for CPB samples.

Figures 9 to 14 show the evolution of MIP porosity of CPB samples while Tables 5 and 6 present respectively the total MIP porosity and the threshold diameter evolution. The comparison between Figures 9 to 14 and Figures 2 to 7 shows that the main differences between CP and CPB results are the height of the maximum mercury intrusions, which are much more important for CPB mixtures (about 10% for CPB compared to about 4% for CP), and the position of the maximum intrusion diameter, of approximately $1 \mu\text{m}$ for all CPB curves (compared to less than $0.1 \mu\text{m}$ for CP samples).

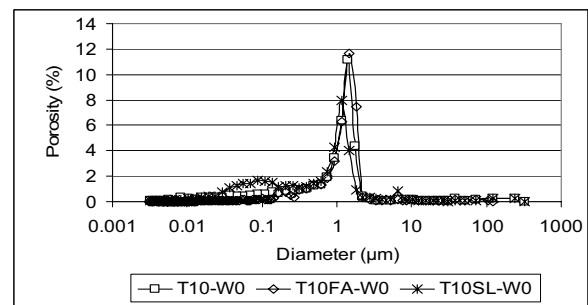


Figure 9, MIP results at 14 days with W0 water

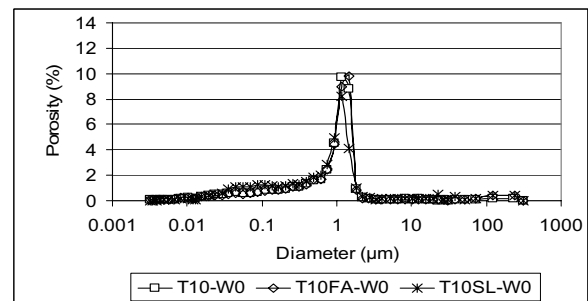


Figure 10, MIP results at 43 days with W0 water

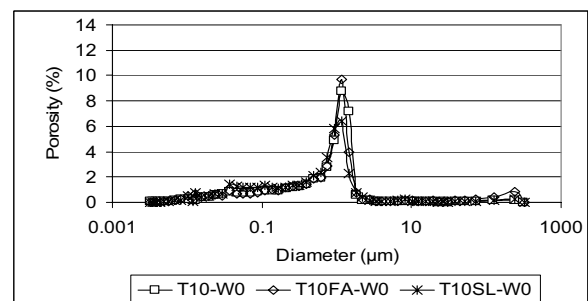


Figure 11, MIP results at 92 days with W0 water

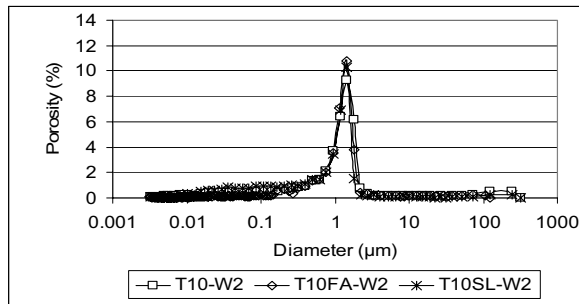


Figure 12, MIP results at 14 days with W2 water

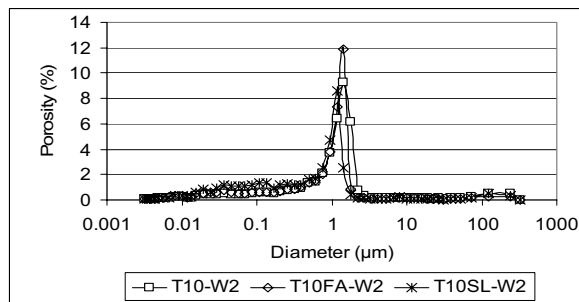


Figure 13, MIP results at 43 days with W2 water

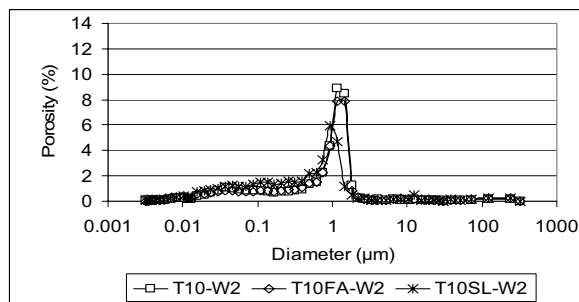


Figure 14, MIP results at 92 days with W2 water

3.2.1 Effect of binders

As observed for CP mixtures, Figures 9 to 14 shows that results for CPB mixtures with T10SL binder are different than the ones for the other two binders. For example, Figure 9 shows that the curves with T10 and T10FA binders have a similar shape; there is only one peak of intrusion at 1 μm and the maximum intrusion takes about 12% of the total porosity. For CPB samples using T10SL binder, the position of the maximum peak is at the left of the other two, being lower at a value of approximately 8% of total porosity. Nevertheless, similar to the CP results, samples using T10SL binder developed a larger proportion of finer porosity than other samples with T10 and T10FA.

3.2.2 Effect of curing time

For similar total porosity of CPB samples (Table 5), a significant decrease in the height of the main intrusion peaks and a movement of the pore size distribution to the left with the curing time is observed, indicating a

refinement of the porosity. On Figures 9 to 11, which show the evolution of MIP porosity for the mixtures using the W0 water, the proportion of the porosity at the maximum rate of intrusion drops from a value of 12% at 14 days to a value lower than 10% after 92 days for T10 and T10FA samples, and from 8% to a value near 6% for the mixture with the T10SL binder. Since the total porosity measured by the MIP technique is unchanged even after a curing time of 92 days, pores of CPB samples become finer with curing time. Another effect of curing time is the decrease of the threshold diameter (Table 6). For T10 and T10FA samples, the threshold diameter moves from about 1.43 μm to about 1.17 μm . This indicates that as these CPB samples evolve, the pores are finer and the pressure to apply to significantly intrude the matrix with mercury increases. The same trend is observed for T10SL samples with water W2; threshold diameters of T10SL samples using W0 and W1 waters remain constant over 92 days.

3.2.3 Effect of mixing water quality

The behaviour of mixtures made with W2 water is similar to the ones with W0 water (see Figures 12 to 14). The pore refinement effect is more apparent at a curing time of 92 days with W2 water. Only the mixture using the T10SL binder and the W2 water has a threshold diameter lower than 1 μm with a value of 0.93 μm at 92 days. A combination of the behaviour of the T10SL binder and a potential precipitation of sulphated minerals in the pores could explain the decrease in bigger pore proportion and the increase of finer pore proportion.

Table 5, CPB's total MIP porosity (%)

	14 days	43 days	92 days
W0-T10	43.99	44.70	44.91
W0-T10FA	45.80	44.85	45.79
W0-T10SL	45.18	45.95	45.03
W1-T10	44.52	43.59	44.94
W1-T10FA	44.16	44.04	44.26
W1-T10SL	44.82	44.34	43.88
W2-T10	44.94	43.80	44.41
W2-T10FA	44.73	43.67	43.63
W2-T10SL	44.52	43.96	45.06

Table 6, CPB's threshold diameters (μm)

	14 days	43 days	92 days
W0-T10	1.4189	1.1729	1.1718
W0-T10FA	1.4378	1.4375	1.165
W0-T10SL	1.1666	1.1653	1.1622
W1-T10	1.4326	1.1716	1.1717
W1-T10FA	1.434	1.1661	1.1663
W1-T10SL	1.1633	1.1647	1.1658
W2-T10	1.4345	1.4387	1.1732
W2-T10FA	1.4348	1.4409	1.1679
W2-T10SL	1.4418	1.1632	0.9283

Figure 15 shows the sum of the porosity with a MIP pore diameter under 0.1 μm at all curing times. Although the results presented are less significant than those for CP mixtures (see Figure 8), it is still the mixture using the T10SL binder and the W2 water that shows the more

important proportion of pores under 0.1 μm at all curing times. Moreover, sulphated water seems to have a beneficial effect on the reduction of the pore size. Except for CPB samples using T10SL and W0 water, all other samples using sulphated water show a higher percentage of small pores than the equivalent control samples using W0 water.

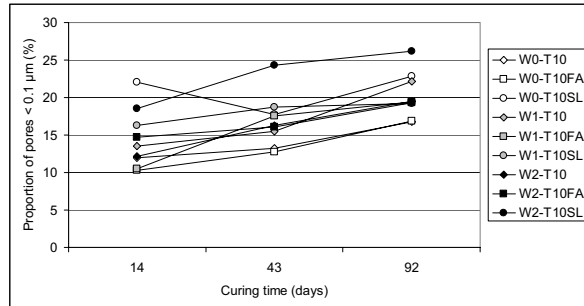


Figure 15, Proportion of pores lower than 0.1 μm .

3.2.4 MIP porosity vs uniaxial compressive strength

Another important aspect of the microstructural behaviour of CPB is the strength development (represented in this study by UCS results). Figure 16 shows the UCS results for CPB samples at the three same curing times (14, 43 and 92 days). Once again as for the MIP tests, the mixtures using the T10 and the T10FA binders have similar behaviour. For these CPB, the UCS typically ranges from 280 kPa at 14 days to about 800 to 1000 kPa at 92 days for the three water types. The strength of mixtures with T10SL binder is higher than those of the other two binders for all samples at all curing times. The highest value is 1822 kPa with water W2 at 92 days, which is in concordance with MIP results that showed a finer porosity for this CPB mixture. Water effects are also present in UCS results. In almost all cases, the sulphated waters gave a better strength than the clean water (W0), supporting the hypothesis that precipitation of sulphate minerals contribute significantly to strength development (Benzaazoua et al., 2004).

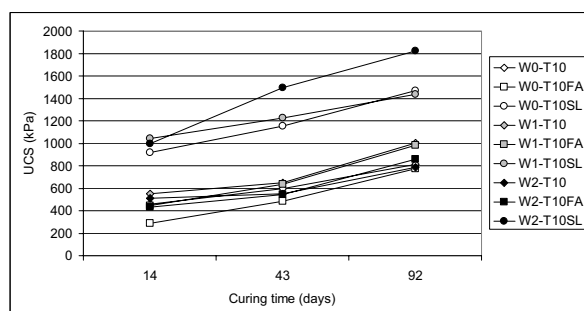


Figure 16, UCS results for CPB samples.

To relate the mechanical strength to the porosity, Figure 17 presents a graph of UCS results against the sum of pore size less than 0.1 μm . The squares represent all results using the T10SL binder and circles represent all results with T10 and T10FA binders (since the study showed that their behaviours are similar). Note that the

grey square is not included in the line equation for T10SL binder. According to this graph, the UCS shows a linear relationship (see Figure 17 for equations) with the proportion of pores less than 0.1 μm and an implicit refinement of pores with the curing time. As the finer pores proportion increases, the UCS increases. For the same proportion of pores < 0.1 μm , the UCS is greater for CPB samples made from T10SL binder. For both relationships, the coefficients of determination are higher than 0.8.

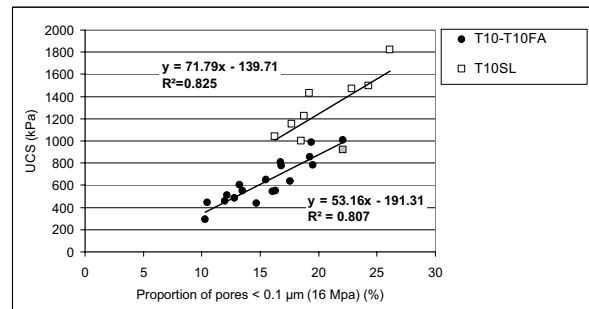


Figure 17, UCS results against proportion of pores size less than 0.1 μm .

4. SUMMARY AND CONCLUSION

This paper showed porosity evolution measured by mercury intrusion porosimetry on cement paste samples and cement paste backfill samples made with ground silica. Three binders were tested: a type 10 Portland cement alone (T10), a mix 20:80 of type 10 Portland cement and blast furnace slag (T10SL) and a mix 70:30 of type 10 Portland cement and fly ash (T10FA). Three different types of water were used in the preparation of the mixtures: a deionised water and two waters coming from two mine backfill plants and containing 4613 and 7549 ppm SO_4^{2-} . The following conclusions can be drawn from this study:

For cement pastes:

- MIP study showed clearly the influence of the binder on the MIP porosity, especially with pore size calculated to be less than 0.01 μm .
- MIP total porosity showed a slight decrease with time for all mixtures and threshold diameter that remained relatively constant for T10 and T10FA binders while it decreased with T10SL mixtures.
- T10SL binder gave finer pores at all curing times compared to pastes with T10 and T10FA binders.
- MIP porosity curves using T10 and T10FA binders were similar for the different curing times and for the different waters.
- Over the curing period of 92 days, waters (W1 and W2) containing sulphate ions up to a value of 7549 ppm induces a finer pore size distribution.
- CP mixtures enhance the impact of ingredients on MIP porosity; the influence factors on CP samples were also observed on CPB samples but to a lesser extent due to the higher w/c ratio.

For cement paste backfills:

- MIP technique allowed comparing porosity evolution for different CPB mixtures.
- Total porosity remained around 44% at all curing times and the threshold diameter decreased with time for all mixtures, indicating a low decrease of pore size.
- For all curing periods and for the studied waters, the sulphated water contributed to the refinement of the porosity and the increase of UCS.
- T10SL binder showed a larger proportion of pore size finer than 0.1 μm and the higher UCS values.
- Microstructural and strength evolution of T10 and T10FA mixtures were similar; replacement of T10 binder by at least 30% of FA could be a good economic opportunity.
- Despite the constant total porosity, MIP results showed that an evolution of pore size finer than 0.1 μm is correlated with UCS evolution.

5. ACKNOWLEDGEMENTS

Funding of this work came from the industrial NSERC Polytechnique-UQAT Chair on Environment and Mine Wastes Management (<http://www.polymtl.ca/enviro-geremi>). This research was also supported by an NSERC Postgraduate Scholarship to the first author.

6. REFERENCES

- Aubertin M, Bussière B, and Bernier L. (2002). Environnement et gestion des résidus miniers. CD, Les Éditions de l'École Polytechnique de Montréal, Montreal, Canada.
- Belem, T., Bussière, B. and Benzaazoua, M. (2001). The effect of microstructural evolution on the physical properties of paste backfill, *Proceedings of Tailings and Mine Waste '01*, Balkema, Rotterdam, ISBN 90 5809 182 1, 365-374.
- Benzaazoua, M., Ouellet, J., Servant, S., Newman, P. and Verburg, R. (1999). Cementitious backfill with high sulfur content Physical, chemical, and mineralogical characterization, *Cement and Concrete Research*, 29, 5, 719-725.
- Benzaazoua, M., Belem, T. and Jolette, D. (2000). Investigation de la stabilité chimique et son impact sur la qualité des remblais miniers cimentés, *Rapport IRSST R-260*, ISBN 2-551-20431-3, 158 p.
- Benzaazoua, M., Fall, M. and Belem, T. (2004). A contribution to understanding the hardening process of cemented pastefill, *Minerals Engineering*, 17, 2, 141-152.
- Chatterji, S. (2001). A discussion of the paper "Mercury porosimetry--an inappropriate method for the measurement of pore size distributions in cement-based materials" by S. Diamond, *Cement and Concrete Research*, 31, 11, 1657-1658.
- Cook, R.A. and Hover, K.C. (1999). Mercury porosimetry of hardened cement pastes, *Cement and Concrete Research*, 29, 6, 933-943.
- Diamond, S. (2000). Mercury porosimetry: An inappropriate method for the measurement of pore size distributions in cement-based materials, *Cement and Concrete Research*, 30, 10, 1517-1525.
- Gallé, C. (2001) Effect of drying on cement-based materials pore structure as identified by mercury intrusion porosimetry: A comparative study between oven-, vacuum-, and freeze-drying, *Cement and Concrete Research*, 31, 10, 1467-1477.
- Gallé, C. (2003). Reply to the discussion by S. Diamond of the paper "Effect of drying on cement-based materials pore structure as identified by mercury intrusion porosimetry: a comparative study between oven-, vacuum- and freeze-drying", *Cement and Concrete Research*, 33, 1, 171-172.
- Hassani, F. and Archibald, J. (1998). Mine backfill CD-ROM, 263 p.
- Hueckel, T., Kaczmarek, M. and Caramuscio P. (1997). Theoretical assessment of fabric and permeability changes in clays affected by organic contaminants, *Canadian Geotechnical Journal*, 34, 588-603.
- Keren, L. and Kajnian, S. (1983). Influence of tailings particles on physical and mechanical properties of fill, *Proceedings of the International Symposium on Mining with Backfill*, Lulea, 7-9 June, 21-29.
- Kjellsen, K.O. (1996). Heat curing and post-heat curing regimes of high-performance concrete: influence on microstructure and C-S-H composition, *Cement and Concrete Research*, 26, 2, 295-307.
- le Roux, K-A (2004). In situ properties and liquefaction potential of cemented paste backfill, Ph. D. thesis to be published, University of Toronto, 183 p.
- Malhotra, V.M. (2001). High-performance high-volume fly ash concrete for sustainability, *Proceedings of the P.-C. Aïtcin symposium on the evolution of concrete technology*, American Concrete Institute, A. Tagnit-Hamou, K.H. Khayat and R. Gagné Eds., 19-74.
- Mitchell, R.J. and Wong, B.C. (1982). Behaviour of cemented tailings sands, *Can. Geotech. J.*, 19, 289-295.
- Neville, A.M. (1981). *Properties of concrete*, third edition, 779 p.
- Ramachandran, V.S. and Beaudoin, J.J. (2001). *Handbook of Analytical Techniques in Concrete Science And Technology*, National Research Council of Canada, Noyes Publications, 985 p.
- Simms P.H. and Yanful E.K. (2001). Measurement and estimation of pore shrinkage and pore distribution in a clayey till during soil-water characteristic curve tests, *Canadian Geotechnical Journal*, 38, 741-754.
- Subauste, J.C. & Odler, I. (2002). Stresses generated in expansive reactions of cementitious systems, *Cement and Concrete Research*, 32, 1, 117-122.
- Winslow, D.N. and Diamond, S. (1970). A mercury porosimetry study of the evolution of porosity in portland cement. *Journal of Materials*, 5, 3, 564-585.
- Wild, S. (2001). A discussion of the paper "Mercury porosimetry--an inappropriate method for the measurement of pore size distributions in cement-based materials" by S. Diamond, *Cement and Concrete Research*, 31, 11, 1653-1654.